

Improvement of Cloud Radiative Forcing and Its Impact on Weather Forecasts

Qiyang Chen^{*1}, Xin-Zhong Liang^{2,3}, Min Xu³, Tiejun Ling⁴ and Julian X.L. Wang⁵

¹National Meteorological Center, China Meteorological Administration, Beijing, China

²Department of Atmospheric and Oceanic Science, University of Maryland, College Park, USA

³Earth System Science Interdisciplinary Center, University of Maryland, College Park, USA

⁴Key Laboratory of Research on Marine Hazards Forecasting, National Marine Environmental Forecasting Center, Beijing, China

⁵Air Resources Laboratory, National Oceanic and Atmospheric Administration, USA

Abstract: The global numerical weather prediction model GRAPES at the National Meteorological Center of the China Meteorological Administration is subject to substantial systematic discrepancies from satellite-retrieved cloud cover, cloud water contents, and radiative fluxes. In particular, GRAPES produces insufficient total cloud cover and liquid water amounts and, consequently, greatly underestimates cloud radiative forcings and causes substantial radiation budget errors. Along with updates of several physics components, new parameterization schemes are incorporated in this study to more realistically represent cloud-radiation interactions. These schemes include predictions for cloud cover, liquid water, and effective radius as well as radiative effects of partial clouds and in-cloud inhomogeneity. As a result, radiation fluxes and cloud radiative forcings at both the surface and top of the atmosphere agree much better with the best available satellite data. The global mean model biases in most radiation fluxes using the new physics are approximately three times smaller than using the original physics. These improvements enhance the model weather forecast skills for key surface variables, including precipitation and 2 m temperature, and for height and temperature in the lower troposphere. Although non-trivial biases still exist, this study nonetheless represents the first essential step toward correcting the radiation imbalance before tackling other formulation deficiencies so that significantly enhanced GRAPES weather forecast skills can eventually be achieved.

Keywords: Cloud inhomogeneity, cloud radiative forcing, fractional cloud, weather forecast.

1. INTRODUCTION

Observational and numerical studies show that clouds play a critical role in the radiation balance of the Earth's climate system. Clouds can cool the Earth by reflecting solar radiation or can warm it by trapping terrestrial radiation [1,2]. Cloud radiative forcing (CRF), defined as the radiative flux difference between total and clear skies, is generally used to quantify the effect of clouds on radiation. Since the 1990s, numerous studies have quantified the essential effects of CRF on the radiation budget and climate [e.g., 3-5]. Compared with transient processes such as the planetary boundary layer and near-surface turbulence exchange, convection, precipitation and advection, radiation transfer has a longer time scale. The importance of radiation and cloud-radiation interactions is generally emphasized in climate prediction. Much less attention has been given to their effects on weather forecasts.

The European Centre for Medium-Range Weather Forecasts (ECMWF) is an exception, emphasizing from its inception the need to incorporate an accurate radiation transfer parameterization in weather forecast models [6,7]. Interactions between radiation and clouds have been continuously improved over the years. Slingo [8] first introduced a diagnostic scheme for fractional cloud cover that depends on relative humidity, stability and convective precipitation rate. Tiedtke [9] then proposed a parameterization to account for the radiative effects of cloud inhomogeneities and convective versus stratiform cloud heterogeneities, which were shown to substantially reduce the model underestimation of net shortwave radiative fluxes at the top of the atmosphere. Morcrette and Jakob [10] later demonstrated the large impact of changing the cloud overlap assumption on radiative fluxes and heating rates. Most recently, Morcrette *et al.* [11] implemented a Monte-Carlo Independent Column Approximation (McICA) method to consider subgrid scale vertical cloud geometric overlapping and horizontal cloud property variability. The latest physical package, which includes the Rapid Radiation Transfer Model (RRTM) plus McICA treatment and MODIS albedo prescriptions, improves the representation of cloud-radiation

*Address correspondence to this author at the National Meteorological Center, China Meteorological Administration, 46 Zhongguancun Nandajie Street, Beijing, China; Tel: 8610 68407472; Fax: 8610 68408706; E-mail: chenqy@cma.gov.cn

interactions. Particularly in the tropics, temperature and wind objective scores are increased through the subsequent reduction of systematic errors in the convection position due to a more realistic vertical distribution of diabatic heating. While smaller, improvement is also seen in the root mean square errors of geopotential height over the globe.

Other operational weather forecast centers have also published works on cloud radiation interactions [e.g., 12-14]. Most of these studies, however, do not address the CRF effects on weather forecast skill. The Global/Regional Assimilation and Prediction System (GRAPES) is a global medium-range weather forecast model being developed by the China Meteorological Administration (CMA). Our initial comparisons with satellite retrievals indicate obvious radiation budget discrepancies, which are mainly caused by GRAPES' underestimation of CRF. Hence, this study focuses on first improving the cloud and radiation parameterization schemes to enhance CRF and then investigating their impacts on weather forecast skills.

Section 2 gives a brief overview of the existing physics representations in GRAPES. Section 3 describes the observational data and model simulations. Section 4 details our new cloud and radiation parameterizations. Section 5 shows the improvements in radiation budget and CRF. Section 6 elaborates the effect of such CRF improvements on weather forecast skill. The results are summarized in section 7.

2. MODEL PHYSICS CONFIGURATION

GRAPES, in its preliminary version, adopts most of its physics schemes from the Weather Research and Forecasting model version 1.3 (WRFv1.3), which includes the Bett-Miller-Janjic (BMJ) cumulus parameterization [15,16], NCEP simple-ice microphysics [17], MRF planetary boundary layer [18], similarity theory surface layer [19], and thermal diffusion land soil [20] schemes. GRAPES also incorporates schemes from the operational ECMWF model in 1989 (Cycle 36) for radiation [21,22] and gravity wave drag [23]. This set of physics schemes is hereafter referred to as the ORG package.

The ORG package is relatively simplistic, as it does not consider important physical processes such as soil moisture and vegetation. The package is also problematic, containing inconsistencies and errors in some schemes and their coupling, especially in cloud-radiation interactions. As a first step, the schemes from WRFv1.3 are replaced by the more comprehensive schemes from WRFv3.1, including the new Kain-Fritsch (Kf) cumulus parameterization [24], NCEP mixed-phase microphysics [17], YSU planetary boundary layer [25], and NOAA land surface model [26,27] schemes. In addition, the RRTM longwave [28] and GSFC shortwave [29] radiation schemes from WRFv3.1 are adopted to replace the ECMWF counterparts. These replacements or updates represent a substantial effort, requiring labor-intensive debugging and testing. More fundamentally, the simple collection of these new schemes does not allow GRAPES to perform better than ORG; in fact, they frequently cause the model to blow up. Therefore, a second, more critical step is taken to develop new cloud and radiation parameterization schemes that consistently integrate these components to achieve the energy balance. These new developments and

their resulting impacts are presented with details in Section 4. This total set of physics schemes is hereafter referred to as the NEW package. Note that the frequent blowup is the very reason for the inability to conduct a parallel sensitivity study to isolate the effects solely from the new cloud and radiation schemes. As such, the study below will focus on comparing overall performance between the NEW and ORG packages as a whole. Some essential sensitivity experiments are included when the specific model configurations allow for a stable integration.

3. OBSERVATIONAL DATA AND MODEL SIMULATIONS

The International Satellite Cloud Climatology Project (ISCCP) provides global distributions of cloud cover, top height, and optical thickness retrieved from thermal infrared and visible radiance measurements [30]. ISCCP's monthly mean D2 product, available at a 2.5° grid spacing [31], is used here to evaluate the predicted cloud cover. Because ground-based observers are better able to detect very low-altitude, highly broken clouds than satellite remote sensors, the global Surface Observations (SOBS) data based on weather reports [32,33] covering December 1982 through November 1991 are also used as a reference for comparison with the predicted low and total cloud amounts. However, surface cloud observations are also subject to specific problems, having poorer quality over lightly traveled ocean regions, such as the southern midlatitudes, than over land. Being formed at low temperatures and under low solar illumination, polar clouds are most challenging for detection [30], and thus, model evaluation must proceed with caution.

Vertically integrated cloud liquid water data are derived from measurements of the Special Sensor Microwave/Imager (SSM/I), whose products are limited to oceans, as the retrievals over land and ice are extremely difficult in the presence of the large variability of surface emissivity. The SSM/I data are available at a 0.25° resolution. ISCCP cloud liquid water at a 2.5° grid spacing are also used for comparison. This comparison provides a measure of observational uncertainty over oceans in mid-low latitudes and is a single set of supplementary data available over land and summer hemisphere high-latitudes where SSM/I values are missing. For warm, nonprecipitating clouds, ISCCP and SSM/I values are consistent in global, zonal, and regional means. For precipitating clouds, however, the ISCCP values are approximately 5-7 times less than the SSM/I values for warm clouds and approximately 2 times less for cold clouds. These value differences are due to the low (high) sensitivity of optical retrievals to large rain (small ice) particles in warm (cold) clouds and the reverse sensitivity for microwave measurements [34].

The Clouds and Earth's Radiant Energy System (CERES) provides the main reference for the radiation budget data in main reference for this study. The CERES FM3 instrument aboard Aqua has an afternoon equatorial crossing time [35]. The retrieved top-of-atmosphere (TOA) fluxes at a 1.875° grid spacing from July 2002 to Oct 2005 for Aqua have been reprocessed to correct for unrealistic global mean net flux imbalances and to fill in missing data [36]. When some components are missing from CERES, monthly mean data

from ISCCP FD-MPF at a 2.5° grid spacing are used as a supplement.

Consistent with the actual forecast operation, GRAPES is integrated for 10 days, starting from 12UTC on each day of July 2005 and January 2006. Because the main results for the different forecast days closely resemble each other and because GRAPES' current usable forecasting length with anomaly correlation coefficients greater than 0.6 is 5 days, only the 5th day forecast is evaluated here. All GRAPES results presented below are monthly mean 5th day forecasts, except for the statistical skill verification, where a daily evaluation is made. In addition, the main conclusions drawn from the results of January are similar to those of July, and hence, the subsequent presentations focus on the latter.

For a direct comparison with the satellite cloud product, the ISCCP simulator is coupled online with GRAPES. The simulator takes the input of cloud and atmospheric conditions and converts them to output that is comparable to the ISCCP data [37, 38]. This paper compares daytime grids of GRAPES with the ISCCP VIS/IR cloud amount (available only in daytime).

4. NEW CLOUD AND RADIATION SCHEMES IMPROVING CRF

As will be discussed in section 5, there are obvious discrepancies in the radiation budget at the TOA and at the surface between the GRAPES forecasts and the satellite retrievals. These discrepancies are mainly caused by substantial underestimates of downwelling surface and upwelling TOA shortwave and longwave CRFs and are identified with much smaller values than observations over most of the globe.

As the first step to resolve such a serious radiation balance problem, CRF is improved by incorporating the following new treatments of cloud-radiation processes within GRAPES: (1) more realistic parameterizations of cloud cover and effective cloud drop size specific to distinct cloud genera; (2) a diagnostic cloud water path calculation based on cloud-resolving model (CRM) simulations and atmospheric radiation measurement (ARM) observations; (3) a scaling factor for the RRTM to consider the longwave effects of fractional rather than binary cloud cover; and (4) a reduction factor for GSFC to account for the within-cloud inhomogeneous effect. These treatments are briefly described below.

4.1. Cloud Cover Parameterization

In the ORG package, clouds in individual layers in each grid are binary: either 1 (total overcast) if the cloud water plus ice content is greater than a threshold of 10^{-6} kg kg⁻¹, or 0 (complete clear sky) otherwise. This approximation may be reasonable when the model resolution is sufficient to resolve clouds. For the present 1° grid, however, fractional cloud cover must be assumed.

The NEW package incorporates the diagnostic cloud cover scheme developed by Liang and Wang [39]. Following Slingo and Slingo [40], four cloud genera are diagnosed: convective (C_c), anvil cirrus (C_i), inversion stratus (C_{is}) and stratiform (C_{st}). For the radiation calculation, C_{st} and C_{is} are combined into a single genus (C_s); C_c forms as a

deep tower penetrating all continuous convective layers, while C_i occupies the top layer of deep convection; and C_{is} occurs in one near-surface layer. Refinements are made for the C_c dependence on convective precipitation after Kiehl *et al.* [41]; the C_i occurrence in the case of a C_c greater than 0.1 and above 650 hPa; the C_{is} dependence on layer stability by Kiehl *et al.* [41] without the pressure factor that accounts for the transition between marine stratus and trade cumulus; and the C_{st} formation in any model layer with a relative humidity exceeding a threshold that decreases from 0.9 at the surface to 0.7 above 800 hPa. As demonstrated by Liang and Wang [39], these refinements substantially reduce model biases in high and total cloud covers and, consequently, the longwave and shortwave radiative forcing in comparison with the ISCCP and ERBE data.

For GRAPES at a 1° grid spacing, it is necessary to make two additional refinements. First, the relative humidity threshold RH_c for the C_{st} formation varies with cloud level pressure p (hPa),

$$RH_c = \begin{cases} 0.8, & \text{when } 125 \leq p \leq 500 \\ 0.6, & \text{when } 500 < p < 750 \\ 0.7, & \text{when } 750 \leq p \leq 900 \end{cases} \quad (1)$$

Second, the C_c maximum is reduced from 0.8 to 0.5, and C_i is calculated by

$$C_i = C_c \leq 0.5, \text{ when } C_c > 0.1 \quad (2)$$

The ORG package prescribes the effective water and ice droplet radius as constants of 10 and 80 μm , respectively. Following Savijarvi *et al.* [42], the effective water droplet radius in the NEW package for a non-precipitating cloud is first calculated in terms of the cloud liquid water content $clwc$ (g m^{-3}),

$$r_{np} = 4 + 7 \min(1.5263, \max(0, clwc)), \quad (3)$$

if over land

$$r_{np} = 5.5 + 9.5 \min(1.5263, \max(0, clwc)), \quad (4)$$

if over ocean

Enhancement due to rain drops is then added below 700 hPa,

$$r_i = (C_c + C_s) / (C_c / r_{cb} + C_s / r_{cs}) \quad (5)$$

where,

$$r_{cb} = r_{np} + 0.6 \min(100, \max(0, 3600P_c)) \quad (6)$$

$$r_{cs} = r_{np} + 1.2 \min(50, \max(0, 3600P_i)), \quad (7)$$

and P_c and P_i are convective and resolved precipitation (m s^{-1}), respectively.

Following Kiehl *et al.* [43], the effective ice droplet radius varies with pressure:

$$r_i = 30 - 20 \max\left(\min\left(\left(p_m / p_s - 0.4\right) / 0.4, 1\right), 0\right), \quad (8)$$

where p_m and p_s are the pressure (hPa) at the center of the model layer and the ground surface, respectively.

Fig. (1) compares the zonal mean cloud cover simulated by GRAPES by using the new versus old cloud schemes against the ISCCP data. Recall that the model outputs are taken from the ISCCP simulator for a consistent comparison. For the total cloud cover (TCC), the ISCCP data have maxima at the equator and the mid-latitudes of both hemispheres, the largest being at 60°S. The old cloud scheme substantially underestimates TCC at all latitudes, amounting only to approximately 25-75% of the ISCCP data. The underestimation is mainly due to the lack of middle (MCC) and low (LCC) cloud cover in most latitudes, especially the MCC in the northern high-latitudes. It is worth mentioning here that the so-called mid-level clouds identified by ISCCP (and simulated with the ISCCP simulator) could also be a combination of semi-transparent high and low clouds whose radiative signatures resemble that of a mid-level cloud. The new cloud scheme significantly increases TCC, MCC and LCC in most latitudes, especially in the tropics and high latitudes.

Fig. (2) compares the zonal mean TCC and LCC with the SOBS surface cloud climatology. The figure shows that the prediction by the new scheme is in good agreement with the SOBS observations, whereas the old scheme contains large errors with substantial underestimations. It should be mentioned that the cloud amount in Fig. (1) is simulated using the ISCCP simulator. Additionally, only daytime GRAPES forecasts are used for the sake of consistency with the ISCCP visible adjusted cloud amounts, which are only available in daytime. Fig. (2) shows the direct output from the model, where both daytime and nighttime forecasts are used, so the curves for the modeled TCC and LCC cloud covers are different in Figs. (1, 2).

4.2. Cloud Water Path Parameterization

The ORG package uses the NCEP simple-ice microphysics scheme to predict cloud water content that directly affects radiation. There are, however, obvious deficiencies in the microphysics scheme that result in a substantial underprediction of cloud water content, especially in the ITCZ. The mixed-phase scheme in the NEW package does not solve this problem. To focus on improving CRF, the radiation and microphysics processes are temporarily decoupled. Specifically, the radiation calculation ignores the prognostic cloud liquid and ice water contents resulting from the NCEP microphysics scheme; instead it uses those of the diagnostic parameterization described below. The solution to the deficiencies in the microphysics scheme will be deferred to future work after addressing the CRF problem, which is among the most fundamental factors for medium-range weather forecasts. Taking this step may cause inconsistency between precipitation and cloud formation, but it will enable us to first address the more serious energy budget issue. The same

approach has been adopted and proved effective in the development of the NCAR climate model [44,45]. Because precipitation and total precipitable water are well predicted by GRAPES, it is advantageous to use a diagnostic scheme to calculate the cloud water path. This study adopts the parameterization developed by Wu and Liang [46] on the basis of the CRM simulations and ARM observations. The use of this diagnostic approach has another advantage in that cloud water content from convection can be readily included. This part of cloud water content is not included in the ORG package as in most existing cumulus parameterization schemes that do not generally predict cloud water content.

The parameterization first calculates the total cloud water path,

$$cwp = clwc_0 \cdot h_i \cdot f(z), \quad (9)$$

where h_i is the scale height; $clwc_0$ is the reference cloud water concentration, and $f(z)$ is the prescribed vertical distribution scaling factor. A regression fitting to the CRM simulations of the ARM measurements leads to,

$$f(z) = \begin{cases} f_1 = e^{-0.378(z/h_i)^2}, & \text{if } z \leq h_i - 500 \\ f_2 = 1.375e^{-0.653(z/h_i)}, & \text{if } z \geq h_i \\ f_3 = f_1 + (z - h_i + 500)(f_2 - f_1) / 500, & \text{if } h_i - 500 < z < h_i \end{cases}, \quad (10)$$

where z is the layer interface height above the surface.

In the original scheme of Wu and Liang (2005), h_i is diagnosed from the column's total precipitable water P (mm):

$$h_i = 700 \ln(1 + P). \quad (11)$$

For the implementation in GRAPES, h_i is set to a constant of 2500 m, and $clwc_0$ is given as 0.30 g m⁻². These choices are made to predict the cloud water path so that it more closely matches the SSM/I measurements. To eliminate the discontinuity in cwp around the new h_i , the following fit function is used,

$$f_1 = e^{-0.333(z/h_i)^2}, \quad (12)$$

Then, the ice content fraction within cloud f_{ice} is determined by temperature,

$$f_{ice} = \begin{cases} 0, & \text{when } T \geq T_0, \text{ or } C_i = 0 \\ 1 - e^{-((T_0 - T)/15)^2}, & \text{when } 233.16 < T < T_0 \\ 1, & \text{when } T < 233.16 \end{cases}, \quad (13)$$

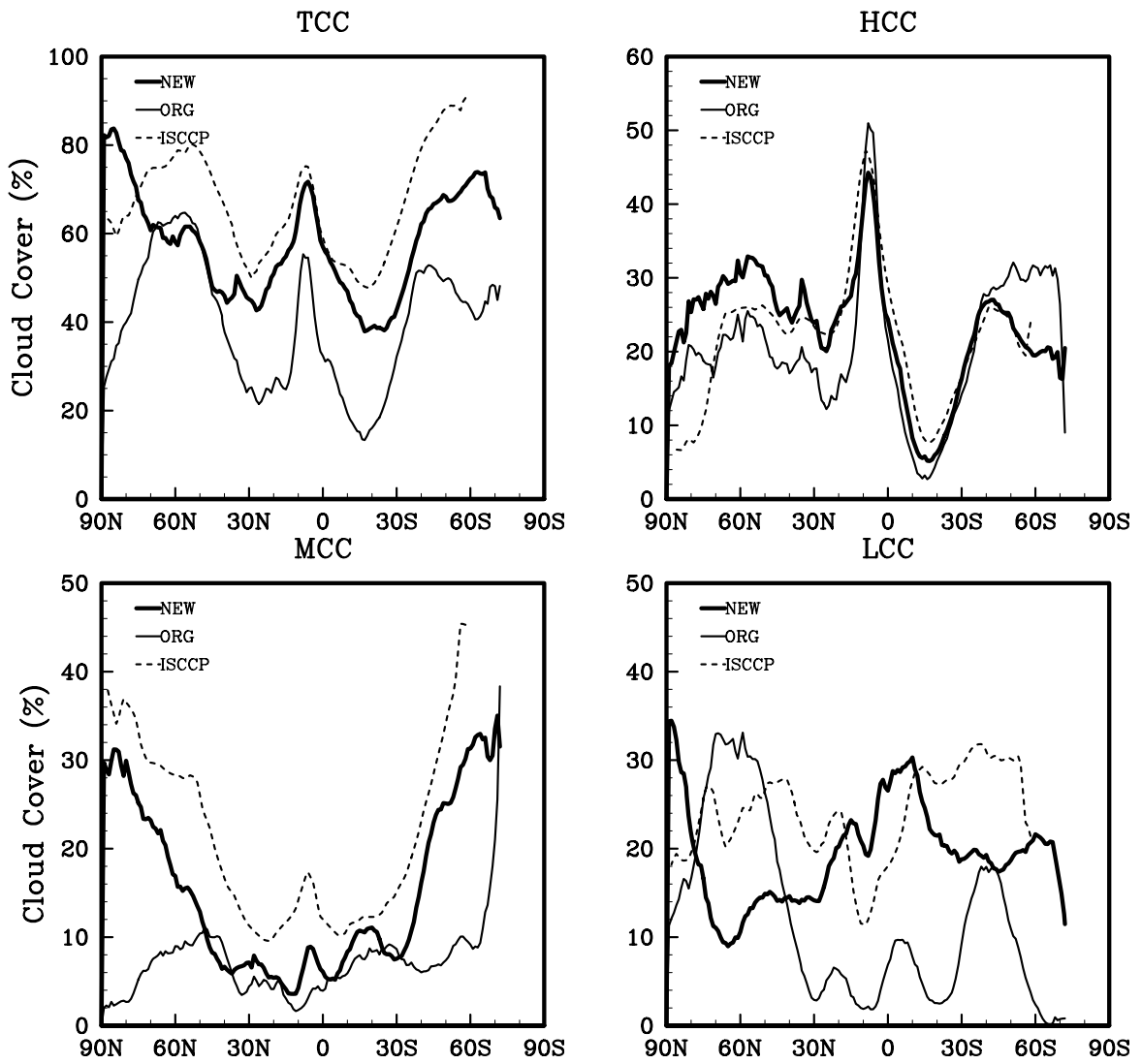


Fig. (1). Zonal mean total (TCC), middle (MCC) and low (LCC) cloud cover (%) from the ISCCP data (dashed) and the 5th-day forecast by GRAPES using the ORG (thin solid) and NEW (thick solid) cloud schemes. Only daytime values are compared.

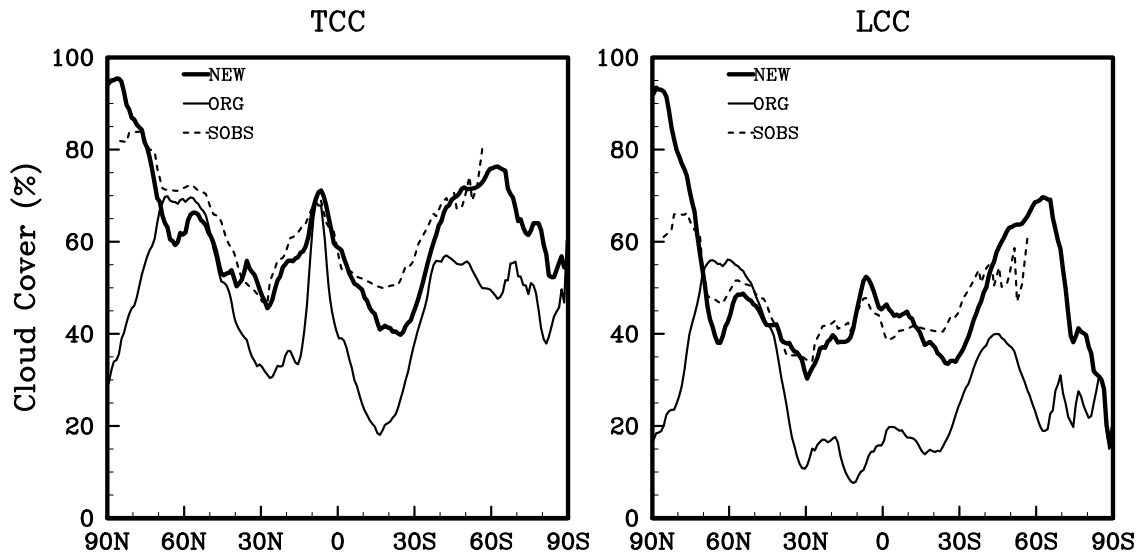


Fig. (2). Zonal mean total (TCC) and low (LCC) cloud cover (%) from the SOBS data (dashed) and the 5th-day forecast by GRAPES using the ORG (thin solid) and NEW (thick solid) cloud schemes.

where T_0 is the temperature threshold for liquid cloud water, set to 263.16 K over land and 269.16 K over ocean, and C_t is the total cloud cover. When the temperature is higher than the threshold, the cloud is in completely liquid form, and f_{ice} is 0; when the temperature is lower than 233.16, the cloud is completely in ice form, and f_{ice} is 1. Now, the cloud ice water path $ciwp$ is calculated by,

$$ciwp = cwp \cdot f_{ice}, \tag{14}$$

and the cloud liquid water path $clwp$ is derived from,

$$clwp = cwp - ciwp. \tag{15}$$

Fig. (3) compares the zonal mean column-total cloud liquid water path (TCW) over oceans with the SSM/I and ISCCP data and the 5th day forecast by GRAPES using the ORG and NEW schemes. The differences between SSM/I and ISCCP are very large. Except over high-latitudes, the ISCCP values are systematically lower than those of SSM/I, although their latitudinal variations are similar. The TCW from SSM/I has its principal peak near 10°N and two secondary maxima in the mid-latitudes of the two hemispheres, with the northern one relatively larger. The forecast by the ORG scheme is very poor, underestimating TCW systematically in all latitudes and having no peak at the equator. The NEW parameterization substantially improves the forecast in almost all latitudes, especially in the tropics and the southern hemisphere.

4.3. Radiation Effect of Fractional Clouds

The RRTM scheme from WRFv3.1 can treat only binary clouds. Any non-zero fractional cloud amount input to radiation will artificially be set to 1. This resetting overestimates the actual cloud effect and, hence, the downwelling longwave flux at the surface compared with the CERES retrievals.

To reduce this deficiency, a scale factor is introduced into the RRTM scheme to enable a fractional cloud effect. First, the maximum cloud cover FCLSCALE in each grid column is calculated and assumed to be the new cloud amount of every vertical layer for this grid column. Then, the grid mean fractional cloud input to the radiation scheme is extended into the full range of FCLSCALE while conserving the production of cloud cover times optical depth. Because FCLSCALE is the maximum amount for all cloudy layers, when the input cloud amount of a layer is less than FCLSCALE, the optical depth per unit area at that layer is attenuated (Fig. 4). Using this approach, the radiative effect of fractional clouds in the first order is incorporated to rectify the overestimation of the cloud effect.

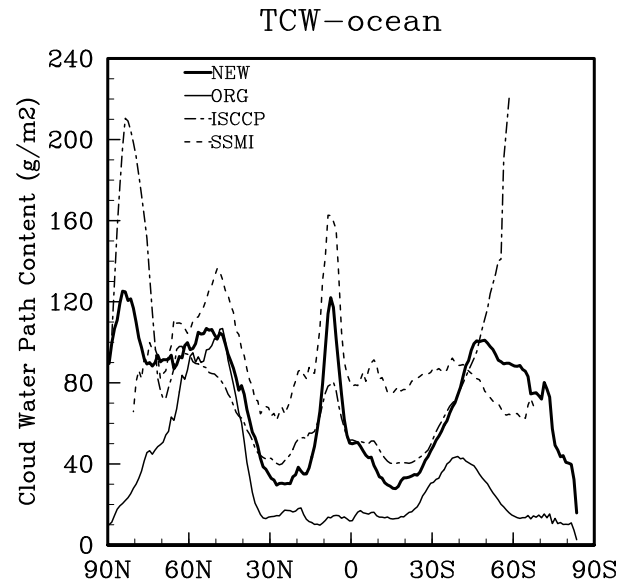


Fig. (3). Zonal mean of global ocean cloud liquid water path (g/m^2) from the SSM/I (dashed) and ISCCP (dot-dashed) data and the 5th-day forecast by GRAPES using the ORG (thin solid) and NEW (thick solid) cloud liquid water path schemes.

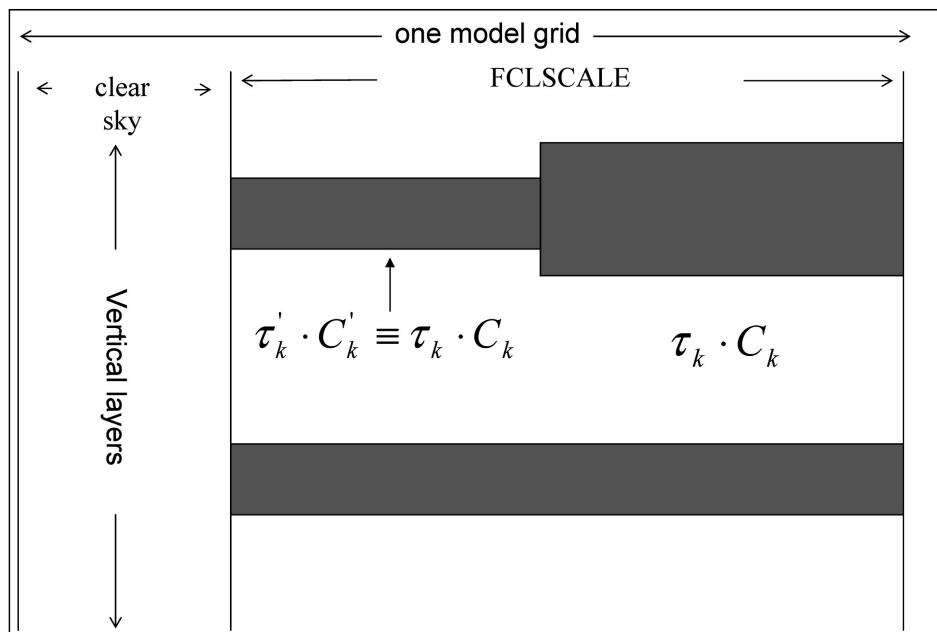


Fig. (4). Illustration of the scaling of fractional cloud effect on radiation by conserving the product of cloud cover times optical depth.

Fig. (5) shows that the scaling largely eliminates the systematic overestimation of downwelling longwave radiation at the surface in the original RRTM scheme, producing a forecast in good agreement with the CERES data. Meanwhile, the net longwave flux at the surface is obviously improved, and downwelling and net shortwave fluxes at the surface as well as upwelling shortwave and longwave fluxes at the TOA become more realistic due to physical interactions (not shown).

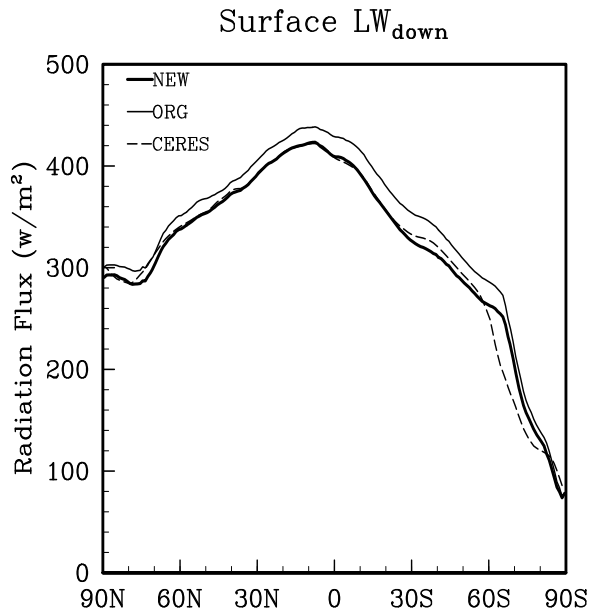


Fig. (5). Zonal mean downwelling longwave radiation flux at the surface of the CERES data (*dashed*) and the 5th-day forecast by GRAPES before (ORG, *thin solid*) and after (NEW, *thick solid*) including the fractional cloud effect.

4.4. Radiative Effect of Cloud Inhomogeneity

The radiative transfer is usually computed once using the profiles of total cloud fraction and in-cloud condensate assuming a homogeneous cloud property distribution. Cahalan *et al.* [47] demonstrate that this assumption overestimates the total cloud albedo because the mean of the logarithm is less than the logarithm of the mean cloud water path. They proposed a reduction factor χ to account for the within-cloud inhomogeneity effect. Afterward, Liang and Wu [48] developed a parameterization from the CRM simulation of ARM measurements,

$$\chi = 0.97 \exp\left[-(f_c - 0.098)^2 / 0.0365\right] + 0.255, \quad (16)$$

where f_c is the cloud cover for individual layers.

This scheme is incorporated into the GSFC shortwave radiation scheme. Note that in the original parameterization of Liang and Wu [48], f_c was defined as the column total cloud fraction. Sensitivity experiments suggest that using f_c for individual layers produces a better result for GRAPES. Fig. (6) shows that the introduction of the reduction factor χ to include the cloud inhomogeneity effect mostly eliminates the underestimation of downwelling shortwave radiation flux

at the surface when the new parameterizations for cloud cover (a) and cloud water path (b) are coupled with the GSFC radiation scheme.

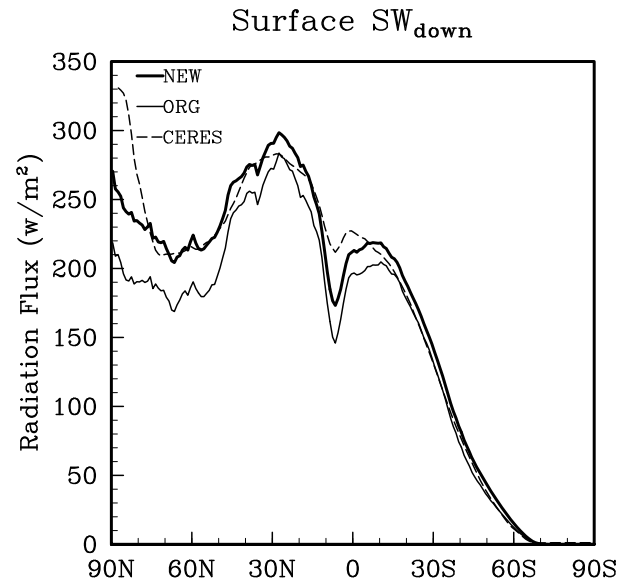


Fig. (6). Zonal mean downwelling shortwave radiation flux at the surface of the CERES data (*dashed*) and the 5th-day forecast by GRAPES before (ORG, *thin solid*) and after (NEW, *thick solid*) including the cloud inhomogeneity effect.

5. IMPROVEMENT OF RADIATION BUDGET

Table 1 lists the global mean radiation budgets for July 2005 from the CERES and ISCCP data and the 5th-day forecasts by GRAPES using the ORG and NEW physics packages. First, the data uncertainty measured as the difference between CERES and ISCCP is generally within 5 W m^{-2} for most radiation components except surface downwelling SW (7 W m^{-2}) and net CRF SW (10 W m^{-2} , not shown).

The ORG package exhibits substantial discrepancies from both the CERES and ISCCP data that are much greater than the data uncertainty. At TOA, the ORG package overestimates the global mean upwelling LW or OLR by 34 W m^{-2} compared with the CERES data. The large bias is caused by the overestimated clear-sky flux and underestimated CRF by 10 and 24 W m^{-2} , respectively. For SW, the net flux is 30 W m^{-2} greater than the CERES data, which is mainly due to an insufficient upwelling CRF.

The surface net LW and SW fluxes are much larger than the observations, by a factor of 1.5 and 1.3 times, respectively. Because errors in upwelling components for both LW and SW are relatively small, the apparent biases in surface net fluxes are mainly from the underestimated downwelling LW (334 versus 353 W m^{-2} of CERES) and the overestimated downwelling SW (231 versus 184 W m^{-2} of CERES). The biases in downwelling LW and SW fluxes at the surface are associated with errors in their corresponding clear-sky fluxes and CRF. For LW, the ORG underestimates the CRF by 14 W m^{-2} and the clear-sky flux by 9 W m^{-2} . For SW, the ORG underestimates the CRF by 30 W m^{-2} , while it overestimates the clear-sky flux by 24 W m^{-2} .

Table 1. Global Mean Radiation Budget Weighted by Area from CERES and ISCCP Data and the 5th-Day Forecast by GRAPES Using the ORG and NEW Physics Packages

	CERES	ISCCP	ORG	NEW
Surface radiation balance ($W m^{-2}$)				
Downwelling LW	353	357	334	365
Net LW	-47	-48	-71	-44
Clear-sky Downwelling LW	--	327	318	333
Upwelling LW CRF	--	2	0	1
Downwelling LW CRF	--	30	16	32
Downwelling SW	184	177	231	182
Net SW	162	160	206	161
Clear-sky Downwelling SW	--	234	258	253
Upwelling SW CRF	--	-5	-3	-7
Downwelling SW CRF	--	-57	-27	-71
TOA radiation balance ($W m^{-2}$)				
OLR	244	240	278	233
Clear-sky Upwelling LW	271	267	281	268
Upward LW CRF	27	27	3	35
Upwelling SW	96	100	66	106
Net SW	235	231	265	225
Clear-sky Upwelling SW	48	50	45	44
Upwelling SW CRF	-48	-50	-21	-62

The clear-sky biases in the ORG downwelling LW and SW fluxes at the surface are quite large. These biases may be the result of the colder modeled atmosphere for LW and the lack of aerosol scattering effects for SW. Further efforts, which are beyond the scope of this study, are needed to reduce the cold biases (e.g., cumulus heating parameterization) and to incorporate the direct and indirect aerosol effects.

Nonetheless, for both the SW and LW net fluxes at the surface and TOA, the substantial discrepancies between GRAPES using the ORG package and the observations are mainly due to underestimation of the corresponding CRF components. The relative CRF contributions to the net LW and SW model errors are 57% and 61% at the surface, respectively, and 71% and 85% at the TOA. As demonstrated in Sections 4a-b, the underestimation of CRF is attributed to an insufficient total cloud cover and cloud water path predicted by the ORG package. After incorporating the refinements, the NEW package increases global mean CRFs systematically and reduces radiation budget biases substantially. The biases in most radiation fluxes with the NEW package, as averaged over the globe, are approximately three times smaller than with the ORG package (Table 1). The zonal mean CRF values in most latitudes at the surface and TOA are greatly increased (Fig. 7), resulting in significantly improved net radiation fluxes (Fig. 8).

6. OVERALL IMPACTS ON WEATHER HINDCASTS

With all the above improvements included, the improved GRAPES (i.e., the version coupling the NEW package) is run for 10-day weather hindcasts every day during July in 2009. The results are compared with those of the original version. As a main concern of forecasters, the geographic distributions of critical near-surface variables, such as precipitation and 2 m temperature, are first evaluated against observations. In addition, the World Meteorological Organization (WMO) has established a set of key statistical verification skill scores to quantify the overall model performance for weather forecasts. This set includes the Anomaly Correlation Coefficient (ACC) and the Root Mean Square Error (RMSE) of geopotential height, temperature and wind verified against the model's analyses. This set also includes the Threat Score (TS) and the Bias (BS) of precipitation compared with the observations. These scores are also compared to depict the gross impacts of the new parameterization schemes on GRAPES' weather forecasting ability. Because the current usable forecast length in GRAPES is 5 days, only the results based on the 5th-day forecasts are shown below, with the major conclusions generally applied for 1- to 4-day forecasts.

6.1. Geographic Distributions of Surface 2 m Temperature and Precipitation

The 5th-day forecasts of the surface 2 m temperature for each day of July with the improved and original versions of GRAPES are averaged separately for comparison with the CRU TS3.0 dataset available at a 0.5° resolution based on an objective analysis of station measurements [49]. For consistent comparison, the GRAPES forecasts are corrected for terrain elevation mismatches between the model and observation data. Fig. (9) compares the forecast errors of GRAPES between using the NEW and ORG packages. Clearly, the NEW package reduces the substantial model errors in northern Asia, Greenland and northern Africa. These broad areas are identified with pronounced cold biases ($4-12^\circ C$) using the ORG package. The new GRAPES largely removes these cold biases, although somewhat overdoing it, resulting in general warm biases. It must be cautioned that the final outcome is complicated by potential problems in other physical processes in addition to cloud-radiation interactions. For example, NOAA has a tendency to produce warm biases [50].

Fig. (10) compares the zonal mean monthly average precipitation of the 5th-day forecast by the improved and original GRAPES with the GPCP analysis, which is available as a $2.5^\circ \times 2.5^\circ$ latitude-longitude grid based on satellite and gauge measurements [51]. Clearly, the improved version reduces the original overestimation of precipitation in the ITCZ by nearly half. The improved version is also closer to GPCP in the southern mid-latitudes, with less rainfall than the original GRAPES.

6.2. Statistical Verification Skill Scores of Geopotential Height, Temperature and Precipitation

Fig. (11) compares the ACC and RMSE of geopotential height and temperature between the improved and original GRAPES forecasts, as verified against the analyses at

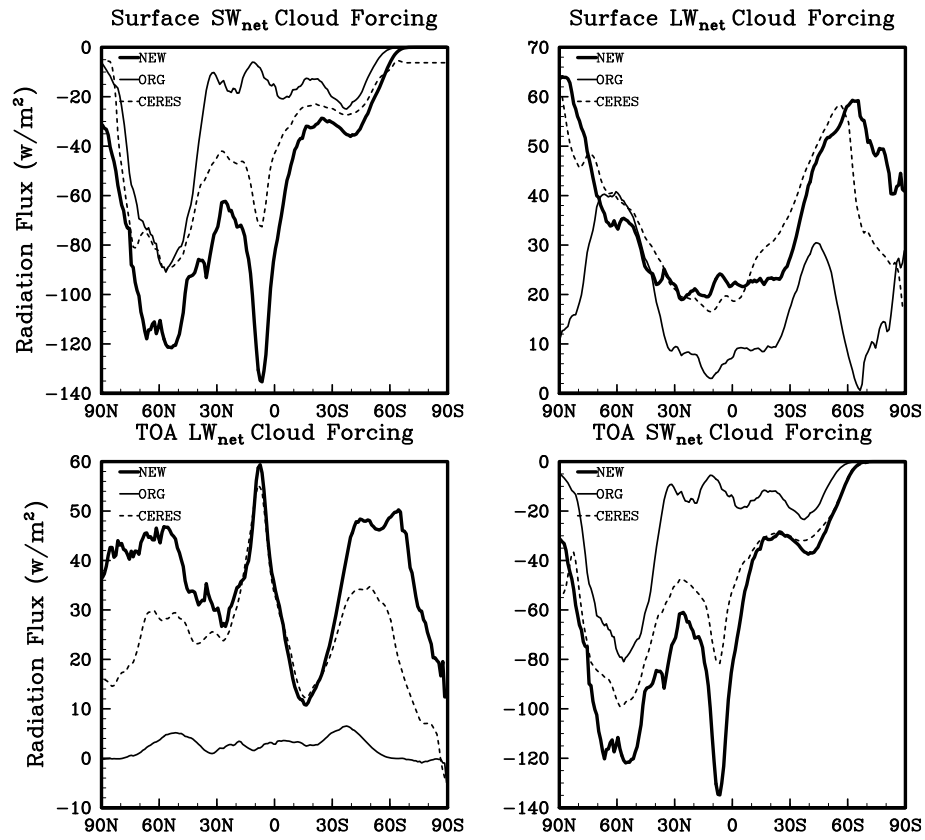


Fig. (7). Zonal mean longwave and shortwave CRF at the surface and TOA of the CERES data (*dashed*) and the 5th-day forecast by GRAPES using the ORG (*thin solid*) and NEW (*thick solid*) schemes.

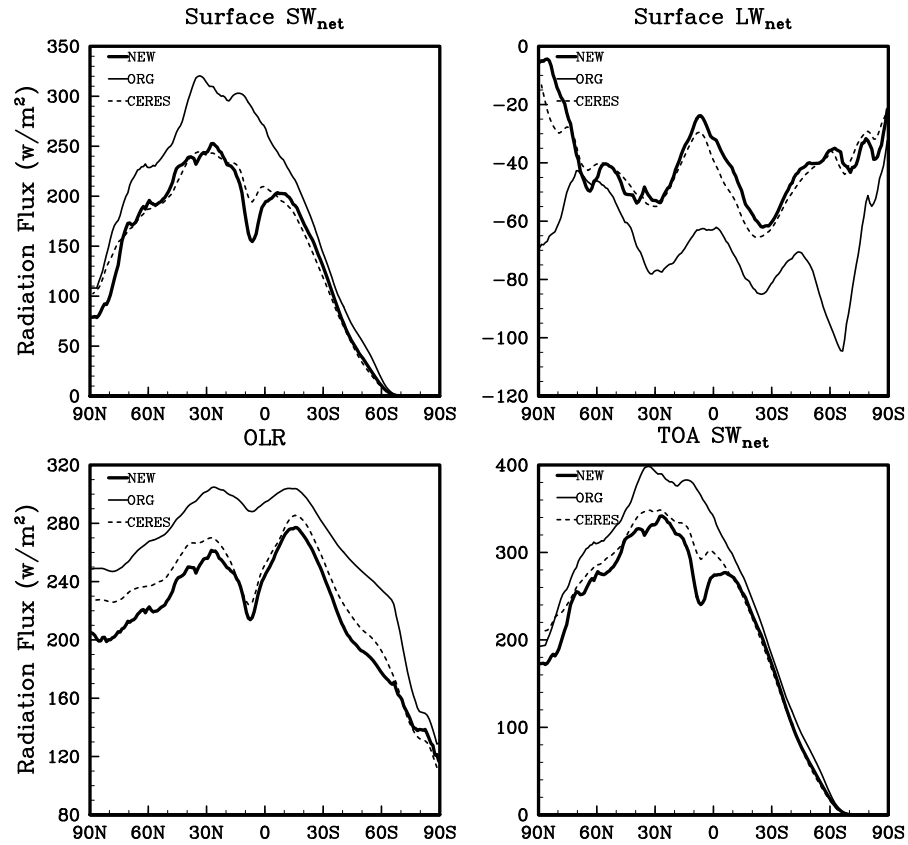


Fig. (8). Zonal mean longwave and shortwave net fluxes at the surface and TOA of the CERES data (*dashed*) and the 5th-day forecast by GRAPES using the ORG (*thin solid*) and NEW (*thick solid*) schemes.

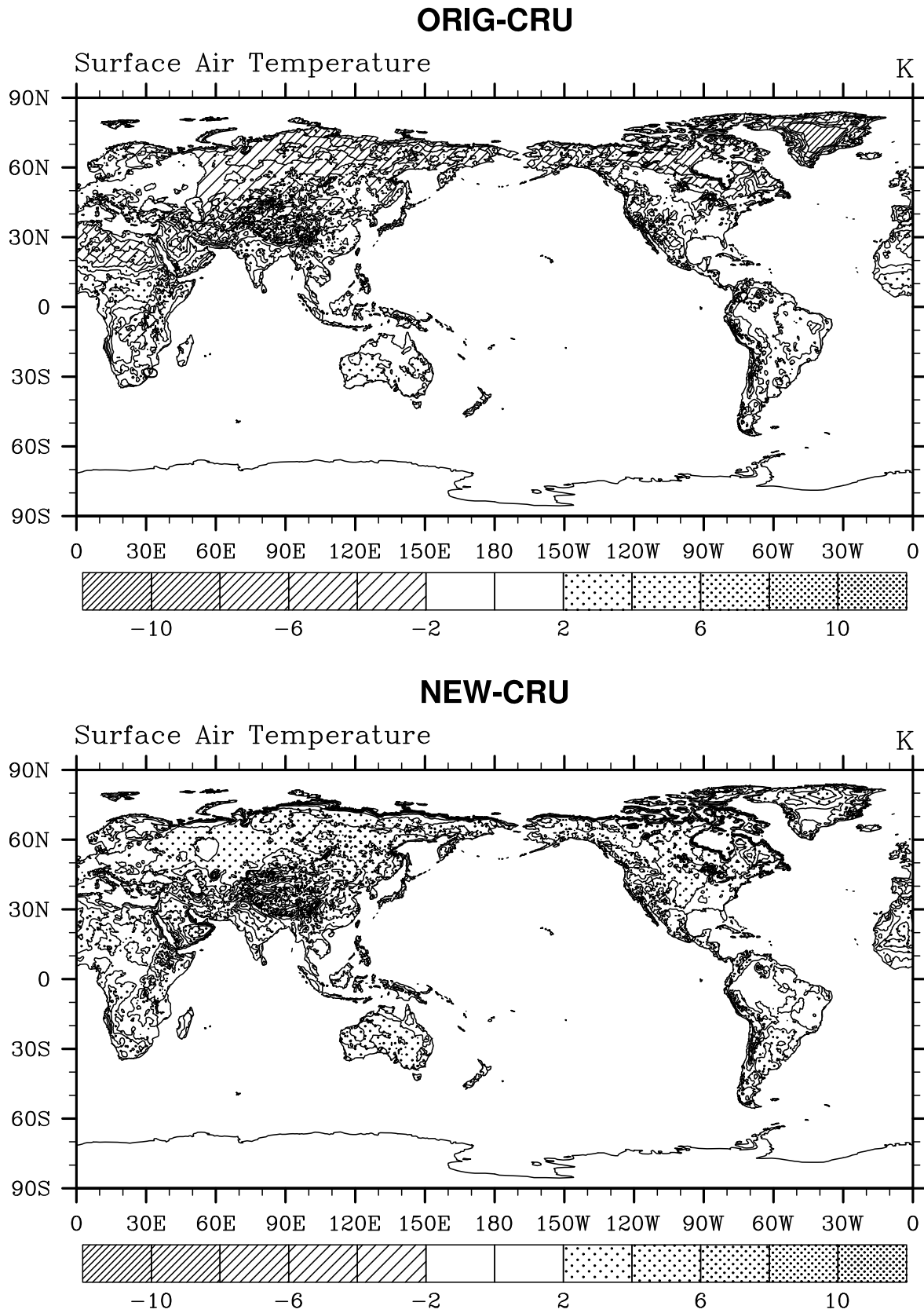


Fig. (9). Surface 2 m temperature errors compared with CRU data for the 5th-day forecast by GRAPES using the ORG and NEW schemes.

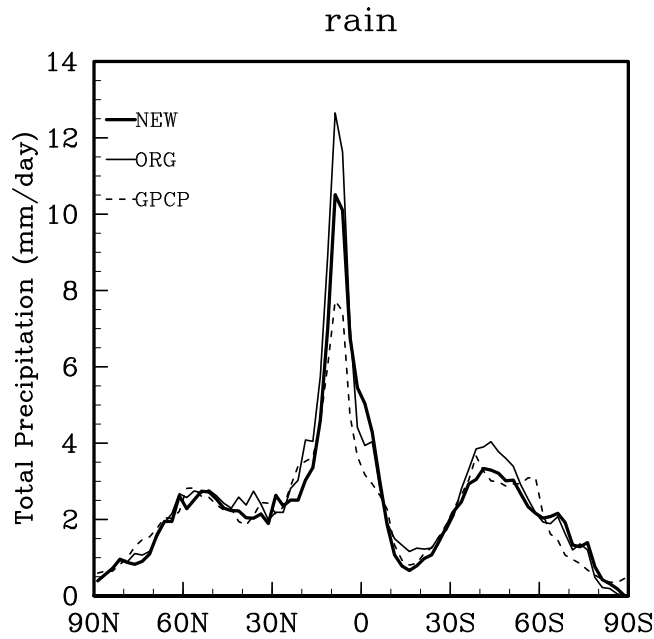


Fig. (10). Zonal mean precipitation of GPCP observational data (dashed) and the 5th-day forecast by GRAPES using the ORG (thin solid) and NEW (thick solid) schemes.

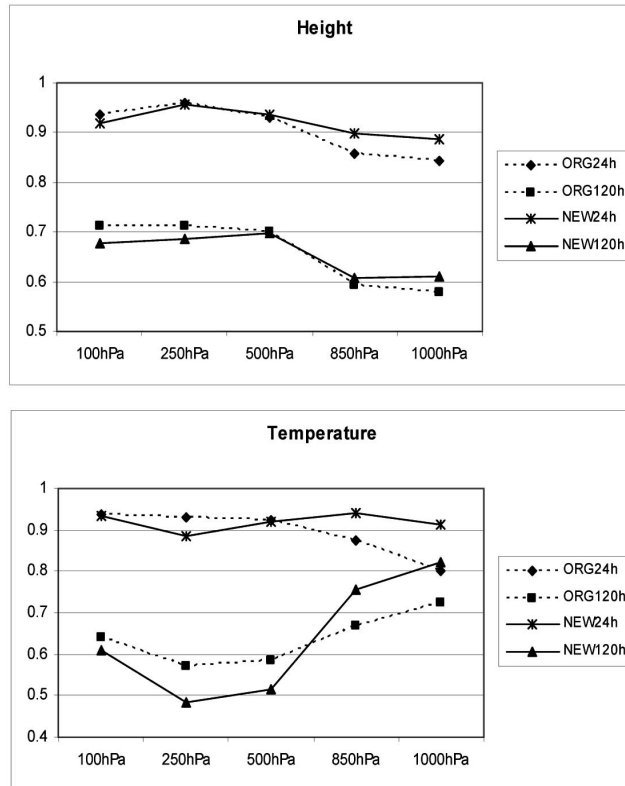


Fig. (11). Anomaly Correlation Coefficient of the 5th-day height and temperature forecasts by GRAPES using the ORG (dashed) and NEW (solid) packages.

5 WMO standard levels from 1000 to 100 hPa to represent low-, medium- and high-level atmospheric circulation. The forecast skills for wind are similar between the two models (not shown). For both short-range (24-hr) and medium-range

(120-hr) forecasts, the new GRAPES obviously increases the skill scores for geopotential height and temperature in the lower troposphere (850 and 1000 hPa). The new GRAPES is less skillful in the upper layers (100 and 250 hPa), especially for temperature. Sensitivity experiments indicate that excessive radiative cooling in the stratosphere and heating at the tropopause are produced in the new GRAPES by inconsistent treatments for the ozone effects in the RRTM LW and GSFC SW schemes¹. The tendency for the RRTM LW scheme to produce systematic cold stratospheric biases has also been identified in the latest 11th Annual WRF User’s Workshop (Boulder, CO, June 21-25, 2010), where a temporal fix was proposed. We will seek a better solution to this problem by using a more comprehensive radiative scheme with consistent LW and SW treatments [50].

Fig. (12) shows the TS of precipitation verified at 400 monitoring stations in China. The verification classifies precipitation into five categories: light, medium, heavy, storm and torrential rainfall, which are defined as accumulated daily amounts greater than 10, 25, 50 and 100 mm, respectively. The higher the TS, the better the forecast. The skills for five forecast time levels, from 36 hours to 120 hours are shown, which indicate that for almost all forecast hours and all precipitation categories, the new GRAPES has superior skills than the original model. In addition, the new GRAPES yields a BS score of precipitation lower than the original model, indicating less false alarms (not shown).

7. SUMMARY AND DISCUSSION

The original GRAPES model produces insufficient cloud cover and cloud water amounts systematically over the globe. Consequently, the model substantially underestimates CRF for both LW and SW downwelling fluxes at the surface and upwelling fluxes at TOA, resulting in severe radiation budget errors and, hence, overall energy balance problems.

To reduce these problems, this study first upgrades several key physics components, including the NOAH (replacing SLAB) land surface model, the NKF (replacing BMJ) cumulus parameterization, the NCEP mixed-phase (replacing simple ice) cloud microphysics scheme, and the RRTM longwave and GSFC shortwave (replacing ECMWF) radiation modules. The upgraded configuration, however, does not solve the problems, and it causes frequent model blowup. Necessarily, then, this study develops new cloud-radiation treatments that is in consistent coupling with the upgrade to improve the CRF representation. These treatments include the following: (1) new schemes for cloud cover, effective cloud droplet size, and cloud water content to provide reasonable cloud properties; (2) a scale factor for the RRTM LW scheme to consider the effect of fractional cloud cover; and (3) a reduction factor for the GSFC SW scheme to account for the within-cloud inhomogeneous effect.

As a result, cloud covers (total, middle, low) are generally increased, especially in the tropics and high latitudes. At the same time, total cloud water amounts are increased in the ITCZ, S.H. mid-latitudes, N.H. high-latitudes and most land areas. Both increases represent improvements, producing a stronger CRF and, hence,

¹At the time this work was completed, these two schemes were the most comprehensive ones available from WRF.

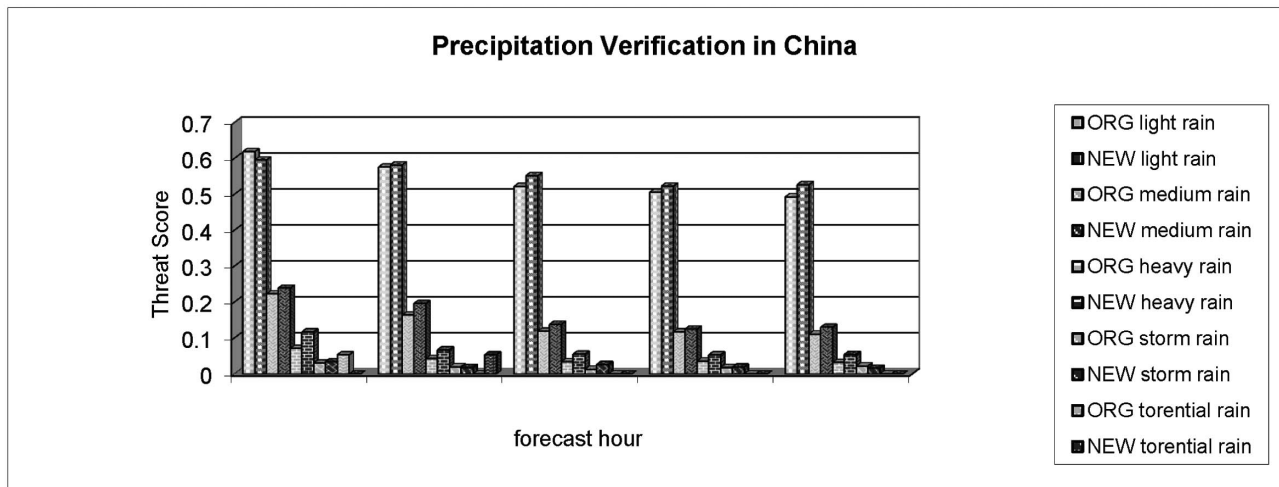


Fig. (12). Precipitation verifications in China of the 5th-day forecast by GRAPES using the ORG and NEW packages.

reducing the severe radiation budget biases in the original GRAPES. The biases in most radiation fluxes with the NEW package, as averaged over the globe, are approximately three times smaller than with the ORG package.

Synoptic evaluation and statistical verification indicate that the new GRAPES, integrating all these refinements, reduces forecast errors for surface 2 m temperature in northern Asia, Greenland and northern Africa, and for precipitation in the ITCZ and South China (not shown). The new GRAPES also improves skill scores for height and temperature in the lower troposphere. The result suggests that CRF is important not only for climate predictions but also for weather forecasts.

Note that the skill enhancement by the new GRAPES is attributed to the integrated improvement of the NEW over the ORG package as a whole. Given the blowup problem, we could not separate the relative contribution from the incorporation of the new cloud-radiation treatments alone versus the other upgraded physics components. Although better radiation budgets at the surface may yield better lower boundary conditions for PBL transport and convection formation, thus affecting precipitation, replacing the BMJ with an NKF cumulus scheme may have a more direct effect on precipitation. However, the rainfall reduction in the ITCZ is not likely due to the cumulus scheme replacement, as a sensitivity experiment showed the opposite: NKF produces more rainfall than BMJ (not shown). Another sensitivity experiment revealed that replacing SLAB with NOAH decreases the precipitation peak in the ITCZ and northern subtropics. This decrease results from the reduced roughness length and turbulent exchange wind speed and thus corrects the overestimation of evaporation and convective precipitation over oceans in the original GRAPES (not shown). However, the improvement of temperature and geopotential height is mainly beneficial from the new cloud-radiation treatments.

Note also that the new GRAPES still contains large cold biases in the stratosphere with opposite warm biases at the tropopause. This deficiency is actually somewhat worsened, resulting in smaller skill scores in the upper troposphere compared with the original model. The problem is identified

with the inability of the current radiation scheme formulation to resolve stratospheric processes. We plan to revisit this problem using the new GRAPES and to seek a solution by incorporating a more comprehensive radiation scheme.

CONFLICT OF INTEREST

The authors confirm that this article content has no conflicts of interest.

ACKNOWLEDGEMENTS

Chen thanks National Key Technologies R & D Program of China (Grant No. 2006BAC02B01) for the financial support and Illinois State Water Survey for hosting her visit and providing facilities to accomplish the work. Liang's effort was partially supported by the U.S. DOE Office of Biological and Environmental Research (BER) DE-SC0001683. The views expressed are those of the authors and do not necessarily reflect those of the sponsoring agencies or the Illinois State Water Survey.

REFERENCES

- [1] Cess RD, Potter GL, Blanchet JP. Intercomparison and interpretation of climate feedback processes in 19 atmospheric general circulation models. *J Geophys Res* 1990; 95: 16, 601-15.
- [2] Stephens GL. Cloud feedbacks in the climate system: a critical review. *J Clim* 2005; 18: 237-73.
- [3] Ramanathan V, Cess R, Harrison E, *et al.* Cloud-radiative forcing and climate: results from the Earth Radiation Budget Experiment. *Science* 1989; 243: 57-63.
- [4] Liang XZ, Wang WC. Cloud overlap effects on general circulation model climate simulations. *J Geophys Res* 1997; 102: 11039-47.
- [5] Zhang MH, Lin WY, Klein SA, *et al.* Comparing clouds and their seasonal variations in 10 atmospheric general circulation models with satellite measurements. *J Geophys Res* 2005; 110: D15S02.
- [6] Geleyn JF. A comprehensive radiation scheme designed for fast computation. Internal Report 8. England: ECMWF Research Dept 1977; p. 36.
- [7] Geleyn JF, Hollingsworth A. An economical analytical method for the computation of the interaction between scattering and line absorption of radiation. *Contrib Atmos Phys* 1979; 52: 1-16.
- [8] Slingo JM. The development and verification of a cloud prediction scheme for the ECMWF model. *Q J R Meteorol Soc* 1987; 113: 899-927.
- [9] Tiedtke M. An extension of cloud-radiation parameterization in the ECMWF model: the representation of subgrid-scale variations of optical depth. *Mon Weather Rev* 1996; 124: 745-50.

- [10] Morcrette JJ, Jakob C. The response of the ECMWF model to changes in the cloud overlap assumption. *Mon Weather Rev* 2000; 128: 1707-32.
- [11] Morcrette, JJ, Barker H, Cole J, *et al.* Impact of a new radiation package, McRad, in the ECMWF Integrated Forecasting System. *Mon Weather Rev* 2008; 136: 4773-98.
- [12] Cullather RI, Harshvardhan K, Campana A. Climatology of cloud and radiation fields in a numerical weather prediction model. *Theor Appl Climatol* 1997; 57: 11-33.
- [13] Rikus L. Application of a Scheme for Validating Clouds in an Operational Global NWP Model. *Mon Weather Rev* 1997; 125: 1615-37.
- [14] Allan RP, Slingo A, Milton SF, *et al.* Evaluation of the Met Office global forecast model using Geostationary Earth Radiation Budget (GERB) data. *Q J R Meteorol Soc* 2007; 133: 1993-2010.
- [15] Betts AK, Miller MJ. A new convective adjustment scheme, Part II: Single column tests using GATE wave, BOMEX, ATEX and arctic air-mass data sets. *Q J R Meteorol Soc* 1986; 112: 693-709.
- [16] Janjic ZI. Comments on "Development and evaluation of a convection scheme for use in climate models". *J Atmos Sci* 2000; 57: 36-86.
- [17] Hong, SY, Juang HMH, Zhao Q. Implementation of prognostic cloud scheme for a regional spectral model. *Mon Weather Rev* 1998; 126: 2621-39.
- [18] Hong SY, Pan HL. Nonlocal boundary layer vertical diffusion in a medium-range forecast model. *Mon Weather Rev* 1996; 124: 2322-39.
- [19] Paulson CA. The mathematical representation of wind speed and temperature profiles in the unstable atmospheric surface layer. *J Appl Meteorol* 1970; 9: 857-61.
- [20] Blackadar A. Modeling pollutant transfer during daytime convection. In: *Proceedings of Fourth symposium on atmospheric turbulence, diffusion and air quality*. Boston: Am Meteorol Soc 1978; 443-7.
- [21] Fouquart Y, Bonnel B. Computations of solar heating of the earth's atmosphere: a new parameterization. *Beitr Phys Atmos* 1980; 53: 35-62.
- [22] Morcrette JJ. Description of the radiation scheme in the ECMWF model. *ECMWF Tech Memo* 1989; 165: p. 26.
- [23] Lott F, Miller MJ. A new subgrid-scale orographic drag parameterization: Its formulation and testing. *Q J R Meteorol Soc* 1997; 123: 101-27.
- [24] Kain JS. The Kain-Fritsch convective parameterization: an update. *J Appl Meteorol* 2004; 43: 170-81.
- [25] Hong SY, Noh Y, Dudhia J. A new vertical diffusion package with an explicit treatment of entrainment processes. *Mon Weather Rev* 2006; 134: 2318-341.
- [26] Chen F, Dudhia J. Coupling an advanced land surface-hydrology model with the Penn State-NCAR MM5 modeling system. Part I: Model implementation and sensitivity. *Mon Weather Rev* 2001; 129: 569-85.
- [27] Ek MB, Mitchell KE, Lin Y, *et al.* Implementation of Noah land surface model advances in the National Centers for Environmental Prediction operational mesoscale Eta model. *J Geophys Res* 2003; 108(D22): 8851.
- [28] Mlawer EJ, Taubman SJ, Brown PD, *et al.* Radiative transfer for inhomogeneous atmosphere: RRTM, a validated correlated-k model for the long-wave. *J Geophys Res* 1997; 102 (D14): 16663-82.
- [29] Chou MD, Suarez MJ. An efficient thermal infrared radiation parameterization for use in general circulation models. *NASA Tech Memo* 104606 1994; pp. 3-5.
- [30] Rossow WB, Schiffer RA. Advances in understanding clouds from ISCCP. *Bull Am Meteorol Soc* 1999; 80: 2261-87.
- [31] Weare B. A comparison of AMIP II model cloud layer properties with ISCCP D2 estimates. *Clim Dyn* 2004; 22: 281-92.
- [32] Warren SG, Hahn CJ, London J, *et al.* Global distribution of total cloud cover and cloud type amounts over land. *NCAR Tech Note, NCAR/TN-273+STR* 1986; p. 29.
- [33] Warren SG, Hahn CJ, London J, *et al.* Global distribution of total cloud cover and cloud type amounts over the ocean. *NCAR Tech Note, NCAR/TN-317+STR* 1988; p. 41.
- [34] Lin B, Rossow WB. Observations of cloud liquid water path over oceans: Optical and microwave remote sensing methods. *J Geophys Res* 1994; 99: 20907-27.
- [35] Wielicki BA, Barkstrom BR, Harrison EF, *et al.* Clouds and the earth's radiant energy system (CERES): an earth observing system experiment. *Bull Am Meteorol Soc* 1996; 77: 853-68.
- [36] Fasullo JT, Trenberth KE. The annual cycle of the energy budget, Part I: Global mean and land-ocean exchanges. *J Clim* 2008; 21: 2297-312.
- [37] Klein SA, Jakob C. Validation and sensitivities of frontal clouds simulated by the ECMWF model. *Mon Weather Rev* 1999; 127: 2514-31.
- [38] Webb M, Senior C, Bony S, *et al.* Combining ERBE and ISCCP data to assess clouds in the Hadley Centre. *ECMWF and LMD atmospheric climate models, Climate Dyn* 2001; 17: 905-22.
- [39] Liang XZ, Wang WC. A GCM study of the climatic effect of 1979-1992 ozone trend. In: *Wang WC, Isaksen ISA, Eds. Atmospheric Ozone as a Climate Gas*. NATO ASI Series. Berlin: Springer-Verlag 1995; pp. 259-88.
- [40] Slingo A, Slingo JM. Response of the National Center for Atmospheric Research Community Climate Model to improvements in the representation of clouds. *J Geophys Res* 1991; 96: 15341-57.
- [41] Kiehl JT, Hack JJ, Briegleb BP. The Simulated earth radiation budget of the NCAR CCM2 and Comparisons with the Earth Radiation Budget Experiment (ERBE). *J Geophys Res* 1994; 99: 20815-27.
- [42] Savijärvi H, Arola A, Räisänen P. Short-wave optical properties of precipitating water clouds. *Q J R Meteorol Soc* 1997; 123: 883-99.
- [43] Kiehl JT, Hack JJ, Bonan GB, *et al.* Description of the NCAR Community Climate Model (CCM3). *NCAR Tech. Note NCAR/TN-420+STR*, 1996; p.143 [Available from Publications Office of NCAR, P.O. Box 3000, Boulder, CO 80307.]
- [44] Kiehl JT, Hack JJ, Bonan GB, *et al.* The National Center for Atmospheric Research Community Climate Model: CCM3. *J Clim* 1998; 11: 1131-49.
- [45] Rasch PJ, Kristjánsson JE. A comparison of the CCM3 model climate using diagnosed and predicted condensate parameterizations. *J Clim* 1998; 11: 1587-614.
- [46] Wu X, Liang XZ. Effect of subgrid cloud-radiation interaction on climate simulations. *Geophys Res Lett* 2005; 32: L24806.
- [47] Cahalan RF, Ridgway W, Wiscombe WJ, *et al.* The albedo of fractal stratocumulus clouds. *Open Atmos Sci J* 1994; 51: 2434-55.
- [48] Liang XZ, Wu X. Evaluation of a GCM subgrid cloud-radiation interaction parameterization using cloud-resolving model simulations. *Geophys Res Lett* 2005; 32: L06801.
- [49] Mitchell TD, Jones PD. An improved method of constructing a database of monthly climate observations and associated high-resolution grids. *Int J Climatol* 2005; 25: 693-712.
- [50] Liang XZ, Xu M, Yuan X, *et al.* Regional climate-weather research and forecasting model (CWRf). *Bull Am Meteorol Soc* 2012; 93: 1363-87.
- [51] Gruber A, Levizzani V. Assessment of global precipitation products: a project of the World Climate Research Programme Global Energy and Water Cycle Experiment (GEWEX) radiation panel. *WCRP Report No. 128, WMO/TD No. 1430*. USA: WMO 2008; p. 50.